

Observation of $B \rightarrow \eta' K^*$ and Evidence for $B^+ \rightarrow \eta' \rho^+$

B. Aubert,¹ R. Barate,¹ M. Bona,¹ D. Boutigny,¹ F. Couderc,¹ Y. Karyotakis,¹ J. P. Lees,¹ V. Poireau,¹
V. Tisserand,¹ A. Zghiche,¹ E. Grauges,² A. Palano,³ J. C. Chen,⁴ N. D. Qi,⁴ G. Rong,⁴ P. Wang,⁴ Y. S. Zhu,⁴
G. Eigen,⁵ I. Ofte,⁵ B. Stugu,⁵ G. S. Abrams,⁶ M. Battaglia,⁶ D. N. Brown,⁶ J. Button-Shafer,⁶ R. N. Cahn,⁶
E. Charles,⁶ M. S. Gill,⁶ Y. Groysman,⁶ R. G. Jacobsen,⁶ J. A. Kadyk,⁶ L. T. Kerth,⁶ Yu. G. Kolomensky,⁶
G. Kukartsev,⁶ G. Lynch,⁶ L. M. Mir,⁶ T. J. Orimoto,⁶ M. Pripstein,⁶ N. A. Roe,⁶ M. T. Ronan,⁶ W. A. Wenzel,⁶
P. del Amo Sanchez,⁷ M. Barrett,⁷ K. E. Ford,⁷ T. J. Harrison,⁷ A. J. Hart,⁷ C. M. Hawkes,⁷ S. E. Morgan,⁷
A. T. Watson,⁷ T. Held,⁸ H. Koch,⁸ B. Lewandowski,⁸ M. Pelizaeus,⁸ K. Peters,⁸ T. Schroeder,⁸ M. Steinke,⁸
J. T. Boyd,⁹ J. P. Burke,⁹ W. N. Cottingham,⁹ D. Walker,⁹ T. Cuhadar-Donszelmann,¹⁰ B. G. Fulsom,¹⁰
C. Hearty,¹⁰ N. S. Knecht,¹⁰ T. S. Mattison,¹⁰ J. A. McKenna,¹⁰ A. Khan,¹¹ P. Kyberd,¹¹ M. Saleem,¹¹
D. J. Sherwood,¹¹ L. Teodorescu,¹¹ V. E. Blinov,¹² A. D. Bukin,¹² V. P. Druzhinin,¹² V. B. Golubev,¹²
A. P. Onuchin,¹² S. I. Serednyakov,¹² Yu. I. Skovpen,¹² E. P. Solodov,¹² K. Yu Todyshev,¹² D. S. Best,¹³
M. Bondioli,¹³ M. Bruinsma,¹³ M. Chao,¹³ S. Curry,¹³ I. Eschrich,¹³ D. Kirkby,¹³ A. J. Lankford,¹³ P. Lund,¹³
M. Mandelkern,¹³ R. K. Mommensen,¹³ W. Roethel,¹³ D. P. Stoker,¹³ S. Abachi,¹⁴ C. Buchanan,¹⁴ S. D. Foulkes,¹⁵
J. W. Gary,¹⁵ O. Long,¹⁵ B. C. Shen,¹⁵ K. Wang,¹⁵ L. Zhang,¹⁵ H. K. Hadavand,¹⁶ E. J. Hill,¹⁶ H. P. Paar,¹⁶
S. Rahatlou,¹⁶ V. Sharma,¹⁶ J. W. Berryhill,¹⁷ C. Campagnari,¹⁷ A. Cunha,¹⁷ B. Dahmes,¹⁷ T. M. Hong,¹⁷
D. Kovalskyi,¹⁷ J. D. Richman,¹⁷ T. W. Beck,¹⁸ A. M. Eisner,¹⁸ C. J. Flacco,¹⁸ C. A. Heusch,¹⁸ J. Kroseberg,¹⁸
W. S. Lockman,¹⁸ G. Nesom,¹⁸ T. Schalk,¹⁸ B. A. Schumm,¹⁸ A. Seiden,¹⁸ P. Spradlin,¹⁸ D. C. Williams,¹⁸
M. G. Wilson,¹⁸ J. Albert,¹⁹ E. Chen,¹⁹ A. Dvoretzskii,¹⁹ F. Fang,¹⁹ D. G. Hitlin,¹⁹ I. Narsky,¹⁹ T. Piatenko,¹⁹
F. C. Porter,¹⁹ A. Ryd,¹⁹ A. Samuel,¹⁹ G. Mancinelli,²⁰ B. T. Meadows,²⁰ K. Mishra,²⁰ M. D. Sokoloff,²⁰ F. Blanc,²¹
P. C. Bloom,²¹ S. Chen,²¹ W. T. Ford,²¹ J. F. Hirschauer,²¹ A. Kreisel,²¹ M. Nagel,²¹ U. Nauenberg,²¹ A. Olivas,²¹
W. O. Ruddick,²¹ J. G. Smith,²¹ K. A. Ulmer,²¹ S. R. Wagner,²¹ J. Zhang,²¹ A. Chen,²² E. A. Eckhart,²²
A. Soffer,²² W. H. Toki,²² R. J. Wilson,²² F. Winklmeier,²² Q. Zeng,²² D. D. Altenburg,²³ E. Feltresi,²³ A. Hauke,²³
H. Jasper,²³ A. Petzold,²³ B. Spaan,²³ T. Brandt,²⁴ V. Klose,²⁴ H. M. Lacker,²⁴ W. F. Mader,²⁴ R. Nogowski,²⁴
J. Schubert,²⁴ K. R. Schubert,²⁴ R. Schwierz,²⁴ J. E. Sundermann,²⁴ A. Volk,²⁴ D. Bernard,²⁵ G. R. Bonneaud,²⁵
P. Grenier,^{25,*} E. Latour,²⁵ Ch. Thiebaux,²⁵ M. Verderi,²⁵ P. J. Clark,²⁶ W. Gradl,²⁶ F. Muheim,²⁶ S. Playfer,²⁶
A. I. Robertson,²⁶ Y. Xie,²⁶ M. Andreotti,²⁷ D. Bettoni,²⁷ C. Bozzi,²⁷ R. Calabrese,²⁷ G. Cibinetto,²⁷ E. Luppi,²⁷
M. Negrini,²⁷ A. Petrella,²⁷ L. Piemontese,²⁷ E. Prencipe,²⁷ F. Anulli,²⁸ R. Baldini-Feroli,²⁸ A. Calcaterra,²⁸
R. de Sangro,²⁸ G. Finocchiaro,²⁸ S. Pacetti,²⁸ P. Patteri,²⁸ I. M. Peruzzi,^{28,†} M. Piccolo,²⁸ M. Rama,²⁸
A. Zallo,²⁸ A. Buzzo,²⁹ R. Capra,²⁹ R. Contri,²⁹ M. Lo Vetere,²⁹ M. M. Macri,²⁹ M. R. Monge,²⁹ S. Passaggio,²⁹
C. Patrignani,²⁹ E. Robutti,²⁹ A. Santroni,²⁹ S. Tosi,²⁹ G. Brandenburg,³⁰ K. S. Chaisanguanthum,³⁰ M. Morii,³⁰
J. Wu,³⁰ R. S. Dubitzky,³¹ J. Marks,³¹ S. Schenk,³¹ U. Uwer,³¹ D. J. Bard,³² W. Bhimji,³² D. A. Bowerman,³²
P. D. Dauncey,³² U. Egede,³² R. L. Flack,³² J. A. Nash,³² M. B. Nikolich,³² W. Panduro Vazquez,³² P. K. Behera,³³
X. Chai,³³ M. J. Charles,³³ U. Mallik,³³ N. T. Meyer,³³ V. Ziegler,³³ J. Cochran,³⁴ H. B. Crawley,³⁴ L. Dong,³⁴
V. Eyges,³⁴ W. T. Meyer,³⁴ S. Prell,³⁴ E. I. Rosenberg,³⁴ A. E. Rubin,³⁴ A. V. Gritsan,³⁵ A. G. Denig,³⁶
M. Fritsch,³⁶ G. Schott,³⁶ N. Arnaud,³⁷ M. Davier,³⁷ G. Grosdidier,³⁷ A. Höcker,³⁷ F. Le Diberder,³⁷ V. Lepeltier,³⁷
A. M. Lutz,³⁷ A. Oyanguren,³⁷ S. Pruvot,³⁷ S. Rodier,³⁷ P. Roudeau,³⁷ M. H. Schune,³⁷ A. Stocchi,³⁷
W. F. Wang,³⁷ G. Wormser,³⁷ C. H. Cheng,³⁸ D. J. Lange,³⁸ D. M. Wright,³⁸ C. A. Chavez,³⁹ I. J. Forster,³⁹
J. R. Fry,³⁹ E. Gabathuler,³⁹ R. Gamet,³⁹ K. A. George,³⁹ D. E. Hutchcroft,³⁹ D. J. Payne,³⁹ K. C. Schofield,³⁹
C. Touramanis,³⁹ A. J. Bevan,⁴⁰ F. Di Lodovico,⁴⁰ W. Menges,⁴⁰ R. Sacco,⁴⁰ G. Cowan,⁴¹ H. U. Flaecher,⁴¹
D. A. Hopkins,⁴¹ P. S. Jackson,⁴¹ T. R. McMahon,⁴¹ S. Ricciardi,⁴¹ F. Salvatore,⁴¹ A. C. Wren,⁴¹ D. N. Brown,⁴²
C. L. Davis,⁴² J. Allison,⁴³ N. R. Barlow,⁴³ R. J. Barlow,⁴³ Y. M. Chia,⁴³ C. L. Edgar,⁴³ G. D. Lafferty,⁴³
M. T. Naisbit,⁴³ J. C. Williams,⁴³ J. I. Yi,⁴³ C. Chen,⁴⁴ W. D. Hulsbergen,⁴⁴ A. Jawahery,⁴⁴ C. K. Lae,⁴⁴
D. A. Roberts,⁴⁴ G. Simi,⁴⁴ G. Blaylock,⁴⁵ C. Dallapiccola,⁴⁵ S. S. Hertzbach,⁴⁵ X. Li,⁴⁵ T. B. Moore,⁴⁵ S. Saremi,⁴⁵
H. Staengle,⁴⁵ R. Cowan,⁴⁶ G. Sciolla,⁴⁶ S. J. Sekula,⁴⁶ M. Spitznagel,⁴⁶ F. Taylor,⁴⁶ R. K. Yamamoto,⁴⁶ H. Kim,⁴⁷
S. E. McIlachlin,⁴⁷ P. M. Patel,⁴⁷ S. H. Robertson,⁴⁷ A. Lazzaro,⁴⁸ V. Lombardo,⁴⁸ F. Palombo,⁴⁸ J. M. Bauer,⁴⁹
L. Cremaldi,⁴⁹ V. Eschenburg,⁴⁹ R. Godang,⁴⁹ R. Kroeger,⁴⁹ D. A. Sanders,⁴⁹ D. J. Summers,⁴⁹ H. W. Zhao,⁴⁹

S. Brunet,⁵⁰ D. Côté,⁵⁰ M. Simard,⁵⁰ P. Taras,⁵⁰ F. B. Viaud,⁵⁰ H. Nicholson,⁵¹ N. Cavallo,^{52, †} G. De Nardo,⁵² F. Fabozzi,^{52, †} C. Gatto,⁵² L. Lista,⁵² D. Monorchio,⁵² P. Paolucci,⁵² D. Piccolo,⁵² C. Sciacca,⁵² M. Baak,⁵³ G. Raven,⁵³ H. L. Snoek,⁵³ C. P. Jessop,⁵⁴ J. M. LoSecco,⁵⁴ T. Allmendinger,⁵⁵ G. Benelli,⁵⁵ K. K. Gan,⁵⁵ K. Honscheid,⁵⁵ D. Hufnagel,⁵⁵ P. D. Jackson,⁵⁵ H. Kagan,⁵⁵ R. Kass,⁵⁵ A. M. Rahimi,⁵⁵ R. Ter-Antonyan,⁵⁵ Q. K. Wong,⁵⁵ N. L. Blount,⁵⁶ J. Brau,⁵⁶ R. Frey,⁵⁶ O. Igonkina,⁵⁶ M. Lu,⁵⁶ R. Rahmat,⁵⁶ N. B. Sinev,⁵⁶ D. Strom,⁵⁶ J. Strube,⁵⁶ E. Torrence,⁵⁶ A. Gaz,⁵⁷ M. Margoni,⁵⁷ M. Morandin,⁵⁷ A. Pompili,⁵⁷ M. Posocco,⁵⁷ M. Rotondo,⁵⁷ F. Simonetto,⁵⁷ R. Stroili,⁵⁷ C. Voci,⁵⁷ M. Benayoun,⁵⁸ J. Chauveau,⁵⁸ H. Briand,⁵⁸ P. David,⁵⁸ L. Del Buono,⁵⁸ Ch. de la Vaissière,⁵⁸ O. Hamon,⁵⁸ B. L. Hartfiel,⁵⁸ M. J. J. John,⁵⁸ Ph. Leruste,⁵⁸ J. Malclès,⁵⁸ J. Ocariz,⁵⁸ L. Roos,⁵⁸ G. Therin,⁵⁸ L. Gladney,⁵⁹ J. Panetta,⁵⁹ M. Biasini,⁶⁰ R. Covarelli,⁶⁰ C. Angelini,⁶¹ G. Batignani,⁶¹ S. Bettarini,⁶¹ F. Bucci,⁶¹ G. Calderini,⁶¹ M. Carpinelli,⁶¹ R. Cenci,⁶¹ F. Forti,⁶¹ M. A. Giorgi,⁶¹ A. Lusiani,⁶¹ G. Marchiori,⁶¹ M. A. Mazur,⁶¹ M. Morganti,⁶¹ N. Neri,⁶¹ E. Paoloni,⁶¹ G. Rizzo,⁶¹ J. J. Walsh,⁶¹ M. Haire,⁶² D. Judd,⁶² D. E. Wagoner,⁶² J. Biesiada,⁶³ N. Danielson,⁶³ P. Elmer,⁶³ Y. P. Lau,⁶³ C. Lu,⁶³ J. Olsen,⁶³ A. J. S. Smith,⁶³ A. V. Telnov,⁶³ F. Bellini,⁶⁴ G. Cavoto,⁶⁴ A. D'Orazio,⁶⁴ D. del Re,⁶⁴ E. Di Marco,⁶⁴ R. Faccini,⁶⁴ F. Ferrarotto,⁶⁴ F. Ferroni,⁶⁴ M. Gaspero,⁶⁴ L. Li Gioi,⁶⁴ M. A. Mazzoni,⁶⁴ S. Morganti,⁶⁴ G. Piredda,⁶⁴ F. Polci,⁶⁴ F. Safai Tehrani,⁶⁴ C. Voena,⁶⁴ M. Ebert,⁶⁵ H. Schröder,⁶⁵ R. Waldi,⁶⁵ T. Adye,⁶⁶ N. De Groot,⁶⁶ B. Franek,⁶⁶ E. O. Olaiya,⁶⁶ F. F. Wilson,⁶⁶ R. Aleksan,⁶⁷ S. Emery,⁶⁷ A. Gaidot,⁶⁷ S. F. Ganzhur,⁶⁷ G. Hamel de Monchenault,⁶⁷ W. Kozanecki,⁶⁷ M. Legendre,⁶⁷ G. Vasseur,⁶⁷ Ch. Yèche,⁶⁷ M. Zito,⁶⁷ X. R. Chen,⁶⁸ H. Liu,⁶⁸ W. Park,⁶⁸ M. V. Purohit,⁶⁸ J. R. Wilson,⁶⁸ M. T. Allen,⁶⁹ D. Aston,⁶⁹ R. Bartoldus,⁶⁹ P. Bechtle,⁶⁹ N. Berger,⁶⁹ R. Claus,⁶⁹ J. P. Coleman,⁶⁹ M. R. Convery,⁶⁹ M. Cristinziani,⁶⁹ J. C. Dingfelder,⁶⁹ J. Dorfan,⁶⁹ G. P. Dubois-Felsmann,⁶⁹ D. Dujmic,⁶⁹ W. Dunwoodie,⁶⁹ R. C. Field,⁶⁹ T. Glanzman,⁶⁹ S. J. Gowdy,⁶⁹ M. T. Graham,⁶⁹ V. Halyo,⁶⁹ C. Hast,⁶⁹ T. Hryn'ova,⁶⁹ W. R. Innes,⁶⁹ M. H. Kelsey,⁶⁹ P. Kim,⁶⁹ D. W. G. S. Leith,⁶⁹ S. Li,⁶⁹ S. Luitz,⁶⁹ V. Luth,⁶⁹ H. L. Lynch,⁶⁹ D. B. MacFarlane,⁶⁹ H. Marsiske,⁶⁹ R. Messner,⁶⁹ D. R. Muller,⁶⁹ C. P. O'Grady,⁶⁹ V. E. Ozcan,⁶⁹ A. Perazzo,⁶⁹ M. Perl,⁶⁹ T. Pulliam,⁶⁹ B. N. Ratcliff,⁶⁹ A. Roodman,⁶⁹ A. A. Salnikov,⁶⁹ R. H. Schindler,⁶⁹ J. Schwiening,⁶⁹ A. Snyder,⁶⁹ J. Stelzer,⁶⁹ D. Su,⁶⁹ M. K. Sullivan,⁶⁹ K. Suzuki,⁶⁹ S. K. Swain,⁶⁹ J. M. Thompson,⁶⁹ J. Va'vra,⁶⁹ N. van Bakel,⁶⁹ M. Weaver,⁶⁹ A. J. R. Weinstein,⁶⁹ W. J. Wisniewski,⁶⁹ M. Wittgen,⁶⁹ D. H. Wright,⁶⁹ A. K. Yarritu,⁶⁹ K. Yi,⁶⁹ C. C. Young,⁶⁹ P. R. Burchat,⁷⁰ A. J. Edwards,⁷⁰ S. A. Majewski,⁷⁰ B. A. Petersen,⁷⁰ C. Roat,⁷⁰ L. Wilden,⁷⁰ S. Ahmed,⁷¹ M. S. Alam,⁷¹ R. Bula,⁷¹ J. A. Ernst,⁷¹ V. Jain,⁷¹ B. Pan,⁷¹ M. A. Saeed,⁷¹ F. R. Wappler,⁷¹ S. B. Zain,⁷¹ W. Bugg,⁷² M. Krishnamurthy,⁷² S. M. Spanier,⁷² R. Eckmann,⁷³ J. L. Ritchie,⁷³ A. Satpathy,⁷³ C. J. Schilling,⁷³ R. F. Schwitters,⁷³ J. M. Izen,⁷⁴ X. C. Lou,⁷⁴ S. Ye,⁷⁴ F. Bianchi,⁷⁵ F. Gallo,⁷⁵ D. Gamba,⁷⁵ M. Bomben,⁷⁶ L. Bosisio,⁷⁶ C. Cartaro,⁷⁶ F. Cossutti,⁷⁶ G. Della Ricca,⁷⁶ S. Dittongo,⁷⁶ L. Lanceri,⁷⁶ L. Vitale,⁷⁶ V. Azzolini,⁷⁷ F. Martinez-Vidal,⁷⁷ Sw. Banerjee,⁷⁸ B. Bhuyan,⁷⁸ C. M. Brown,⁷⁸ D. Fortin,⁷⁸ K. Hamano,⁷⁸ R. Kowalewski,⁷⁸ I. M. Nugent,⁷⁸ J. M. Roney,⁷⁸ R. J. Sobie,⁷⁸ J. J. Back,⁷⁹ P. F. Harrison,⁷⁹ T. E. Latham,⁷⁹ G. B. Mohanty,⁷⁹ M. Pappagallo,⁷⁹ H. R. Band,⁸⁰ X. Chen,⁸⁰ B. Cheng,⁸⁰ S. Dasu,⁸⁰ M. Datta,⁸⁰ K. T. Flood,⁸⁰ J. J. Hollar,⁸⁰ P. E. Kutter,⁸⁰ B. Mellado,⁸⁰ A. Mihalys,⁸⁰ Y. Pan,⁸⁰ M. Pierini,⁸⁰ R. Prepost,⁸⁰ S. L. Wu,⁸⁰ Z. Yu,⁸⁰ and H. Neal⁸¹

(The BABAR Collaboration)

¹Laboratoire de Physique des Particules, F-74941 Annecy-le-Vieux, France

²Universitat de Barcelona, Facultat de Física Dept. ECM, E-08028 Barcelona, Spain

³Università di Bari, Dipartimento di Fisica and INFN, I-70126 Bari, Italy

⁴Institute of High Energy Physics, Beijing 100039, China

⁵University of Bergen, Institute of Physics, N-5007 Bergen, Norway

⁶Lawrence Berkeley National Laboratory and University of California, Berkeley, California 94720, USA

⁷University of Birmingham, Birmingham, B15 2TT, United Kingdom

⁸Ruhr Universität Bochum, Institut für Experimentalphysik 1, D-44780 Bochum, Germany

⁹University of Bristol, Bristol BS8 1TL, United Kingdom

¹⁰University of British Columbia, Vancouver, British Columbia, Canada V6T 1Z1

¹¹Brunel University, Uxbridge, Middlesex UB8 3PH, United Kingdom

¹²Budker Institute of Nuclear Physics, Novosibirsk 630090, Russia

¹³University of California at Irvine, Irvine, California 92697, USA

¹⁴University of California at Los Angeles, Los Angeles, California 90024, USA

¹⁵University of California at Riverside, Riverside, California 92521, USA

¹⁶University of California at San Diego, La Jolla, California 92093, USA

¹⁷University of California at Santa Barbara, Santa Barbara, California 93106, USA

¹⁸University of California at Santa Cruz, Institute for Particle Physics, Santa Cruz, California 95064, USA

¹⁹California Institute of Technology, Pasadena, California 91125, USA

- ²⁰University of Cincinnati, Cincinnati, Ohio 45221, USA
²¹University of Colorado, Boulder, Colorado 80309, USA
²²Colorado State University, Fort Collins, Colorado 80523, USA
²³Universität Dortmund, Institut für Physik, D-44221 Dortmund, Germany
²⁴Technische Universität Dresden, Institut für Kern- und Teilchenphysik, D-01062 Dresden, Germany
²⁵Ecole Polytechnique, Laboratoire Leprince-Ringuet, F-91128 Palaiseau, France
²⁶University of Edinburgh, Edinburgh EH9 3JZ, United Kingdom
²⁷Università di Ferrara, Dipartimento di Fisica and INFN, I-44100 Ferrara, Italy
²⁸Laboratori Nazionali di Frascati dell'INFN, I-00044 Frascati, Italy
²⁹Università di Genova, Dipartimento di Fisica and INFN, I-16146 Genova, Italy
³⁰Harvard University, Cambridge, Massachusetts 02138, USA
³¹Universität Heidelberg, Physikalisches Institut, Philosophenweg 12, D-69120 Heidelberg, Germany
³²Imperial College London, London, SW7 2AZ, United Kingdom
³³University of Iowa, Iowa City, Iowa 52242, USA
³⁴Iowa State University, Ames, Iowa 50011-3160, USA
³⁵Johns Hopkins University, Baltimore, Maryland 21218, USA
³⁶Universität Karlsruhe, Institut für Experimentelle Kernphysik, D-76021 Karlsruhe, Germany
³⁷Laboratoire de l'Accélérateur Linéaire, IN2P3-CNRS et Université Paris-Sud 11, Centre Scientifique d'Orsay, B.P. 34, F-91898 ORSAY Cedex, France
³⁸Lawrence Livermore National Laboratory, Livermore, California 94550, USA
³⁹University of Liverpool, Liverpool L69 7ZE, United Kingdom
⁴⁰Queen Mary, University of London, E1 4NS, United Kingdom
⁴¹University of London, Royal Holloway and Bedford New College, Egham, Surrey TW20 0EX, United Kingdom
⁴²University of Louisville, Louisville, Kentucky 40292, USA
⁴³University of Manchester, Manchester M13 9PL, United Kingdom
⁴⁴University of Maryland, College Park, Maryland 20742, USA
⁴⁵University of Massachusetts, Amherst, Massachusetts 01003, USA
⁴⁶Massachusetts Institute of Technology, Laboratory for Nuclear Science, Cambridge, Massachusetts 02139, USA
⁴⁷McGill University, Montréal, Québec, Canada H3A 2T8
⁴⁸Università di Milano, Dipartimento di Fisica and INFN, I-20133 Milano, Italy
⁴⁹University of Mississippi, University, Mississippi 38677, USA
⁵⁰Université de Montréal, Physique des Particules, Montréal, Québec, Canada H3C 3J7
⁵¹Mount Holyoke College, South Hadley, Massachusetts 01075, USA
⁵²Università di Napoli Federico II, Dipartimento di Scienze Fisiche and INFN, I-80126, Napoli, Italy
⁵³NIKHEF, National Institute for Nuclear Physics and High Energy Physics, NL-1009 DB Amsterdam, The Netherlands
⁵⁴University of Notre Dame, Notre Dame, Indiana 46556, USA
⁵⁵Ohio State University, Columbus, Ohio 43210, USA
⁵⁶University of Oregon, Eugene, Oregon 97403, USA
⁵⁷Università di Padova, Dipartimento di Fisica and INFN, I-35131 Padova, Italy
⁵⁸Universités Paris VI et VII, Laboratoire de Physique Nucléaire et de Hautes Energies, F-75252 Paris, France
⁵⁹University of Pennsylvania, Philadelphia, Pennsylvania 19104, USA
⁶⁰Università di Perugia, Dipartimento di Fisica and INFN, I-06100 Perugia, Italy
⁶¹Università di Pisa, Dipartimento di Fisica, Scuola Normale Superiore and INFN, I-56127 Pisa, Italy
⁶²Prairie View A&M University, Prairie View, Texas 77446, USA
⁶³Princeton University, Princeton, New Jersey 08544, USA
⁶⁴Università di Roma La Sapienza, Dipartimento di Fisica and INFN, I-00185 Roma, Italy
⁶⁵Universität Rostock, D-18051 Rostock, Germany
⁶⁶Rutherford Appleton Laboratory, Chilton, Didcot, Oxon, OX11 0QX, United Kingdom
⁶⁷DSM/Dapnia, CEA/Saclay, F-91191 Gif-sur-Yvette, France
⁶⁸University of South Carolina, Columbia, South Carolina 29208, USA
⁶⁹Stanford Linear Accelerator Center, Stanford, California 94309, USA
⁷⁰Stanford University, Stanford, California 94305-4060, USA
⁷¹State University of New York, Albany, New York 12222, USA
⁷²University of Tennessee, Knoxville, Tennessee 37996, USA
⁷³University of Texas at Austin, Austin, Texas 78712, USA
⁷⁴University of Texas at Dallas, Richardson, Texas 75083, USA
⁷⁵Università di Torino, Dipartimento di Fisica Sperimentale and INFN, I-10125 Torino, Italy
⁷⁶Università di Trieste, Dipartimento di Fisica and INFN, I-34127 Trieste, Italy
⁷⁷IFIC, Universitat de Valencia-CSIC, E-46071 Valencia, Spain
⁷⁸University of Victoria, Victoria, British Columbia, Canada V8W 3P6
⁷⁹Department of Physics, University of Warwick, Coventry CV4 7AL, United Kingdom
⁸⁰University of Wisconsin, Madison, Wisconsin 53706, USA
⁸¹Yale University, New Haven, Connecticut 06511, USA

(Dated: July 28, 2018)

We present an observation of $B \rightarrow \eta' K^*$. The data sample corresponds to 232 million $B\bar{B}$ pairs collected with the BABAR detector at the PEP-II asymmetric-energy B Factory at SLAC. We measure the branching fractions (in units of 10^{-6}) $\mathcal{B}(B^0 \rightarrow \eta' K^{*0}) = 3.8 \pm 1.1 \pm 0.5$ and $\mathcal{B}(B^+ \rightarrow \eta' K^{*+}) = 4.9^{+1.9}_{-1.7} \pm 0.8$, where the first error is statistical and the second systematic. A simultaneous fit results in the observation of $B \rightarrow \eta' K^*$ with $\mathcal{B}(B \rightarrow \eta' K^*) = 4.1^{+1.0}_{-0.9} \pm 0.5$. We also search for $B \rightarrow \eta' \rho$ and $\eta' f_0(980)(f_0 \rightarrow \pi^+ \pi^-)$ with results and 90% confidence level upper limits $\mathcal{B}(B^+ \rightarrow \eta' \rho^+) = 8.7^{+3.1+2.3}_{-2.8-1.3} (< 14)$, $\mathcal{B}(B^0 \rightarrow \eta' \rho^0) < 3.7$, and $\mathcal{B}(B^0 \rightarrow \eta' f_0(980)(f_0 \rightarrow \pi^+ \pi^-)) < 1.5$. Charge asymmetries in the channels with significant yields are consistent with zero.

PACS numbers: 13.25.Hw, 11.30.Er

Decays of B mesons involving the flavor-changing neutral current transition $b \rightarrow s$ are an important place to search for evidence of physics beyond the Standard Model. A comparison of the amplitude $\sin 2\beta$ of time-dependent CP violation in the neutral CP eigenstates $J/\psi K_S^0$ and $\eta' K_S^0$ provides one of the most sensitive tests [1]. In order to unambiguously interpret the time-dependent CP violation measurement in $\eta' K_S^0$ it is important to understand the full set of underlying amplitudes by making measurements of branching fractions in the $\eta' K^*$ decays.

In B decays to final states comprising $\eta^{(*)} K^{(*)}$ the final states $\eta' K^*$ and ηK are suppressed, and the final states $\eta' K$ and ηK^* are enhanced. Two explanations of the experimentally observed pattern differ substantially in the details of the suppression for $B \rightarrow \eta' K^*$ [2, 3]. From previous experimental data and flavor SU(3) arguments it is expected that the branching fractions for $B \rightarrow \eta' K^*$ are less than 10^{-5} [4]. The related decays $B \rightarrow \eta' \rho$ occur via CKM suppressed tree diagrams and are expected to be small. Theoretical approaches using QCD factorization [5] and perturbative QCD [6] predict branching fractions for $B^+ \rightarrow \eta' \rho^+$ of $6\text{--}9 \times 10^{-6}$ and for $B^0 \rightarrow \eta' \rho^0$ of $0.5\text{--}2 \times 10^{-7}$.

In this Letter, we present searches for $B \rightarrow \eta' K^*$, $B \rightarrow \eta' \rho$ and $B^0 \rightarrow \eta' f_0(980)(f_0 \rightarrow \pi^+ \pi^-)$, which shares the same final state as $B^0 \rightarrow \eta' \rho^0$. Throughout this Letter, charge conjugation is implied. Results are obtained from unbinned, extended maximum likelihood (ML) fits to data collected with the BABAR detector at the PEP-II asymmetric e^+e^- collider located at the Stanford Linear Accelerator Center. The BABAR detector and relevant details specific to this analysis are described elsewhere [7, 8]. The analysis uses 211 fb^{-1} of data recorded at the $\Upsilon(4S)$ resonance, corresponding to 232 million $B\bar{B}$ pairs, and closely follows the approach described in Ref. [8].

We select η' , K^* , ρ , η , K_S^0 and π^0 candidates through the decays $\eta' \rightarrow \eta\pi^+\pi^-$ ($\eta'_{\pi\pi}$), $\eta' \rightarrow \rho^0\gamma$ ($\eta'_{\rho\gamma}$), $K^{*0} \rightarrow K^+\pi^-$, $K^{*+} \rightarrow K_S^0\pi^+$ ($K_{K_S^0\pi^+}^{*+}$), $K^{*+} \rightarrow K^+\pi^0$ ($K_{K^+\pi^0}^{*+}$), ρ^0 (and f_0) $\rightarrow \pi^+\pi^-$, $\rho^+ \rightarrow \pi^+\pi^0$, $\eta \rightarrow \gamma\gamma$, $K_S^0 \rightarrow \pi^+\pi^-$ and $\pi^0 \rightarrow \gamma\gamma$. We impose the following requirements on candidate invariant masses, in MeV/c^2 : $910 < (m_{\eta\pi\pi}, m_{\rho\gamma}) < 1000$ for η' , $755 < m_{K\pi} < 1035$ for the K^* , $510 < m_{\pi\pi^0} < 1070$ for ρ^+ and $510 < m_{\pi\pi} < 1060$ for ρ^0 (f_0), $490 < m_{\gamma\gamma} < 600$ for η ,

$486 < m_{\pi\pi} < 510$ for K_S^0 and $120 < m_{\gamma\gamma} < 150$ for π^0 . For the masses of the η' , K^* and ρ , which will be included as observables in the ML fit described below, the selection is wide enough to allow for a parameterization of the background. For K_S^0 candidates we require a flight distance of at least three times its estimated uncertainty.

We also use the helicity-frame decay angle θ_H of K^* , ρ , and $f_0(980)$. The helicity frame is defined as the vector meson rest frame with polar axis along the direction of the boost from the B rest frame. The angle θ_H is the angle between the polar axis and the flight direction of the charged resonance daughter. For K^{*0} and ρ^0 the kaon candidate and the positively charged pion, respectively, are used to define that angle. We use mode dependent selection criteria on $\cos \theta_H$, with the lower bound between -0.95 and -0.70 and the upper bound of either 0.95 or 1.00 . Decay modes suffering from higher combinatoric background due to low momentum pions have the tighter cuts applied. The helicity has a $\cos^2 \theta_H$ distribution for K^* and ρ signal events and is flat for the $f_0(980)$.

All charged pion candidates are required to have particle identification (PID) consistent with pions and inconsistent with protons, kaons, and electrons. No such requirement is made of K_S^0 daughters. Charged kaon candidates are required to have PID consistent with kaons and inconsistent with pions, protons and electrons.

We form B meson candidates by combining an η' candidate with either a K^* or ρ candidate. B meson candidates are characterized kinematically by the energy substituted mass, $m_{\text{ES}} = (s/4 - \mathbf{p}_B^2)^{1/2}$ and the energy difference $\Delta E = E_B - \sqrt{s}/2$ where (E_B, \mathbf{p}_B) is the four-momentum of the B candidate, expressed in the $\Upsilon(4S)$ frame and \sqrt{s} is the e^+e^- center of mass energy. Signal events peak at zero for ΔE and at the B mass for m_{ES} , with typical resolutions of 20 MeV and $3.0 \text{ MeV}/c^2$, respectively. We require $5.25 \leq m_{\text{ES}} \leq 5.29 \text{ GeV}/c^2$ for all modes, $-0.2 \leq \Delta E \leq 0.150 \text{ GeV}$ for modes where the vector meson decay includes a neutral pion and $-0.2 \leq \Delta E \leq 0.125 \text{ GeV}$ otherwise.

Backgrounds arise primarily from random combinations of particles in continuum $e^+e^- \rightarrow q\bar{q}$ ($q = u, d, s, c$) events. To reject these events, we employ the angle θ_T in the $\Upsilon(4S)$ frame between the thrust axis of the B candidate's daughters and that of the remaining particles in the event. Continuum events are produced well

above threshold, with a jet-like topology resulting in a distribution of $|\cos\theta_T|$ that is sharply peaked near 1 for candidates formed in such events. Events containing true $\Upsilon(4S)$ decays are produced near threshold with particles distributed isotropically, resulting in a uniform distribution of $|\cos\theta_T|$. We require $|\cos\theta_T| < 0.9$ for decays with $\eta'_{\pi\pi}$, and $|\cos\theta_T| < 0.75$ for the higher-background $\eta'_{\rho\gamma}$ decays. Due to large backgrounds in $\eta'_{\rho\gamma}$, we only use the $\eta'_{\pi\pi}$ decay in reconstructing $B \rightarrow \eta'\rho/f_0(980)$.

Additional discrimination against continuum background occurs in the ML fit and is provided by a Fisher discriminant, \mathcal{F} . This is a linear combination of discriminating variables with weights chosen to maximize the separation between signal and continuum background. \mathcal{F} contains the angles of the B momentum and B thrust axis with respect to the beam axis, the B -flavor tagging category [9], and the zeroth and second angular moment of the energy flow in the rest of the event with respect to the B candidate thrust axis [8].

After selection, events containing multiple B candidates occur less than 30% of the time. In such cases, we choose the B candidate with the η' mass closest to the Particle Data Group (PDG) value [10].

We use Monte Carlo (MC) simulation [11] for an initial survey of background from $B\bar{B}$ events and to identify for detailed study any decays that are not rejected by candidate selection. The remaining background is composed almost entirely of charmless resonant B decays, especially $B \rightarrow \eta'K$. We account for B backgrounds by including in the ML fit an additional component which models these charmless, resonant decays. Backgrounds arising from charmed B decays have been studied and found to be negligible or accounted for by our continuum background model. Backgrounds from non-resonant B decays have been found to be consistent with zero.

We determine yields and charge asymmetries ($\mathcal{A}_{ch} = (n^+ - n^-)/(n^+ + n^-)$) for each decay chain from a ML fit with the observables ΔE , m_{ES} , \mathcal{F} , $m_{\eta'}$, the mass of the candidate vector meson m_V , and $\mathcal{H} \equiv \cos\theta_H$. For charged (neutral) B decays, n^\pm is defined as the number of B^\pm decays (final states with K^\pm). For each event i and hypothesis j (signal, continuum, $B\bar{B}$), we define the probability density function (PDF) as a simple product of the individual observable PDFs:

$$\mathcal{P}_j^i = \mathcal{P}_j(m_{ES}^i) \mathcal{P}_j(\Delta E^i) \mathcal{P}_j(\mathcal{F}^i) \mathcal{P}_j(m_{\eta'}^i) \mathcal{P}_j(m_V^i) \mathcal{P}_j(\mathcal{H}^i).$$

For the $\eta'\pi^+\pi^-$ final state, a fourth hypothesis is added to account explicitly for a possible $\eta'f_0$ signal.

The total likelihood function is then given by

$$\mathcal{L} = \frac{\exp(-\sum_j n_j)}{N!} \prod_i \left(\sum_j n_j \mathcal{P}_j^i \right),$$

where N is the number of events in the sample and n_j is the yield of events of hypothesis j to be found by maximizing \mathcal{L} . In addition to the yields and \mathcal{A}_{ch} for each

hypothesis, parameters describing the continuum PDFs are also allowed to vary (see below).

We parameterize the PDFs for peaking observables with either a single or asymmetric Gaussian, sum of two Gaussians, or a Breit-Wigner as required. Slowly varying observables are described by low degree polynomials or phase-space motivated functions [8]. Several PDFs require linear combinations of peaking and non-peaking shapes. We parameterize the $f_0(980)$ mass and width using measured values [12].

For the signal and $B\bar{B}$ background components we determine the PDF parameters from simulation. Control samples with topologies similar to our signal (e.g., $B^- \rightarrow D^0\pi^-$) are used to verify and adjust simulated resolutions [8]. For the continuum background we obtain initial PDF parameters from data excluding the ΔE and m_{ES} signal region (sideband). We further refine the continuum PDFs by letting as many parameters as feasible vary in the fit to the full data. The final fitted continuum background PDF parameters are found to be in close agreement with their initial values.

We apply several tests to the fitting procedure for validation before implementing it on the data. In particular, we evaluate any possible bias in our event yields due to our neglect of small correlations between the observables, which our PDFs ignore by construction. We determine the bias by fitting ensembles of simulated continuum experiments generated from the PDF into which we embed the expected number of signal and $B\bar{B}$ background events randomly taken from samples of fully simulated MC events. Measured correlations in the sideband data (pure $q\bar{q}$) are found to be small. The measured biases for each decay chain are given in Table I.

We compute the branching fraction for each decay by subtracting the fit bias from the measured yield and dividing the result by the efficiency (determined from simulation and ancillary studies), the product of the daughter branching fractions, and the number of produced $B\bar{B}$ pairs. We assume equal decay rates of the $\Upsilon(4S)$ to B^+B^- and $B^0\bar{B}^0$. In Table I we show for each decay the measured branching fraction, event yield, efficiency and daughter branching fraction as well as \mathcal{A}_{ch} .

Measurements for separate decay chains are combined by adding the values of $-2\ln\mathcal{L}$ as functions of branching fraction, taking appropriate account of correlated and uncorrelated systematic uncertainties (described below) [8]. The significance is taken as the square root of the difference between the value of $-2\ln\mathcal{L}$ (including systematics) for zero signal and the minimum. For modes where the combined significance is less than 4 standard deviations, we quote 90% confidence level (C.L.) upper limits. We compute these as the branching fraction below which lies 90% of the total likelihood integral in the positive branching fraction domain.

For modes with evidence of a signal, we show in Fig. 1 projections onto m_{ES} and ΔE of subsamples (containing

TABLE I: Summary of results showing (from left): fitted signal yield n before bias correction, fit bias, detection efficiency ε , product daughter branching fraction $\prod \mathcal{B}_i$ [10], significance S (including systematic uncertainties) in standard deviations, measured branching fraction \mathcal{B} and signal charge asymmetry \mathcal{A}_{ch} for each mode. The values in parentheses are 90% C.L. upper limits. The result for $B^0 \rightarrow \eta' f_0(980)(f_0 \rightarrow \pi^+ \pi^-)$ includes the branching fraction for $f_0 \rightarrow \pi^+ \pi^-$, which is not well known. Results in bold face represent combined fits to multiple decay chains (when present).

Mode	n (ev.)	Bias (ev.)	$\varepsilon(\%)$	$\prod \mathcal{B}_i(\%)$	$S(\sigma)$	$\mathcal{B}(10^{-6})$	\mathcal{A}_{ch}
$B \rightarrow \eta' K^*$					5.6	$4.1^{+1.0}_{-0.9} \pm 0.5$	
$B^0 \rightarrow \eta' K^{*0}$					4.3	$3.8 \pm 1.1 \pm 0.5$	$-0.08 \pm 0.25 \pm 0.02$
$\eta'_{\eta\pi\pi} K^{*0}$	$22.6^{+7.7}_{-6.7}$	$+1.7 \pm 0.9$	19.0 ± 1.2	11.6	3.9	$4.1^{+1.5}_{-1.3}$	
$\eta'_{\rho\gamma} K^{*0}$	$35.1^{+14.2}_{-12.7}$	$+9.5 \pm 4.8$	16.9 ± 1.1	19.7	2.0	$3.3^{+1.9}_{-1.6}$	
$B^+ \rightarrow \eta' K^{*+}$					3.6	$4.9^{+1.9}_{-1.7} \pm 0.8 (< 7.9)$	$0.30^{+0.33}_{-0.37} \pm 0.02$
$\eta'_{\eta\pi\pi} K^{*+}_{K^0\pi^+}$	$11.2^{+5.7}_{-4.5}$	$+0.8 \pm 0.5$	18.0 ± 1.2	4.0	3.2	$6.2^{+3.4}_{-2.7}$	
$\eta'_{\rho\gamma} K^{*+}_{K^0\pi^+}$	$14.8^{+11.2}_{-9.7}$	$+2.9 \pm 1.5$	15.8 ± 1.1	6.8	1.2	$4.7^{+4.5}_{-3.9}$	
$\eta'_{\eta\pi\pi} K^{*+}_{K^+\pi^0}$	$5.2^{+5.4}_{-3.6}$	$+1.0 \pm 0.5$	10.7 ± 0.6	5.8	1.2	$2.9^{+3.7}_{-2.6}$	
$\eta'_{\rho\gamma} K^{*+}_{K^+\pi^0}$	$3.1^{+12.1}_{-9.6}$	-2.3 ± 1.3	8.0 ± 0.5	9.8	0.5	$2.9^{+6.7}_{-5.4}$	
$B^0 \rightarrow \eta' \rho^0$	$14.9^{+10.6}_{-8.4}$	$+11.2 \pm 5.7$	22.8 ± 1.4	17.5	0.3	$0.4^{+1.2+1.6}_{-0.9-0.6} (< 3.7)$	
$B^0 \rightarrow \eta' f_0(\rightarrow \pi^+ \pi^-)$	$-2.6^{+6.0}_{-4.0}$	-3.8 ± 2.0	25.4 ± 1.6	17.5	0.2	$0.1^{+0.6+0.9}_{-0.4-0.4} (< 1.5)$	
$B^+ \rightarrow \eta' \rho^+$	$57.3^{+16.0}_{-14.7}$	$+11.5 \pm 5.8$	13.0 ± 1.0	17.5	3.2	$8.7^{+3.1+2.3}_{-2.8-1.3} (< 14)$	$-0.04 \pm 0.28 \pm 0.02$

63 – 85% of all signal events) enriched by a requirement on the ratio of the signal likelihood to the total likelihood. The likelihood is computed excluding the plotted variable. Figure 2 shows background-subtracted distributions of the K^{*0} mass and helicity obtained with the sPlot technique described in [13]. These plots illustrate that the $K\pi$ signal we observe is consistent with the $K^*(892)$ and is polarized as one would expect in a pseudoscalar-vector B decay.

Systematic uncertainties in this analysis are dominated by our knowledge of signal and $B\bar{B}$ background PDF modeling, along with the fit bias and the efficiencies of the track and neutral particle selections. Uncertainty due to continuum PDF modeling is largely incorporated into the statistical uncertainty since most continuum background parameters are allowed to vary in the fit. Uncertainties in the signal PDF parameters are estimated from comparisons between data and MC in control samples. Varying the signal PDF parameters within these errors results in a mode dependent variation in signal yield of between 0.1 and 1.6 events.

The uncertainty in the fit bias is taken to be half of the correction. We estimate the uncertainty from $B\bar{B}$ modeling by taking half of the difference between the signal yield fitted with and without the $B\bar{B}$ component (0.2 to 10 events). The uncertainty due to non-resonant $B\bar{B}$ background is estimated by taking half the difference between the signal yield in the nominal fit and in a fit in which a non-resonant background component has been added (0.7 to 4.8 events). Uncertainties in reconstruction efficiency are determined from supplementary studies of

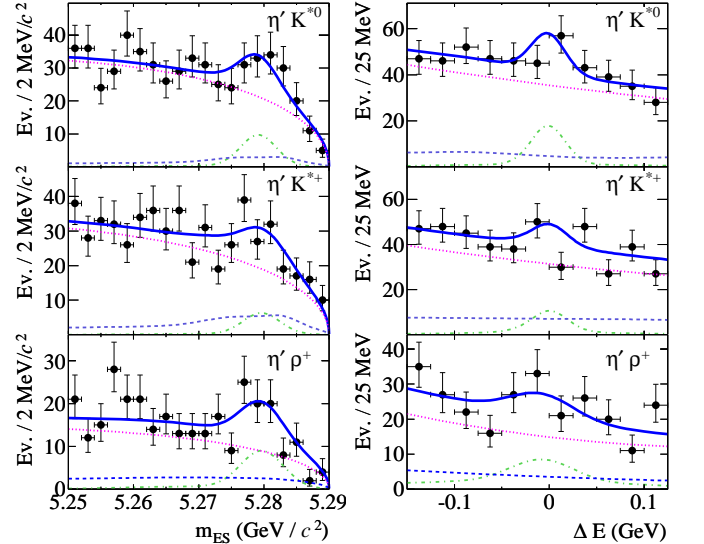


FIG. 1: (Color online) B candidate m_{ES} (left) and ΔE (right) projections obtained with a cut on the likelihood (see text) for $B^0 \rightarrow \eta' K^{*0}$ (top), $B^+ \rightarrow \eta' K^{*+}$ (middle) and $B^+ \rightarrow \eta' \rho^+$ (bottom). Submodes have been combined. The data are represented by points with uncertainties, full fit functions by solid curves, $B\bar{B}$ background by dashed, continuum by dotted and signal by dot-dashed curves. Depending on the decay, the plots contain 63 – 85% of all signal events.

control samples. These include 0.8% per charged track (excluding daughters of the K_s^0), 1.5% per photon, and 1.9% for a K_s^0 . The systematic uncertainty in the number of $B\bar{B}$ pairs is 1.1% [14]. Published data [10] provide the uncertainties in the B -daughter product branching

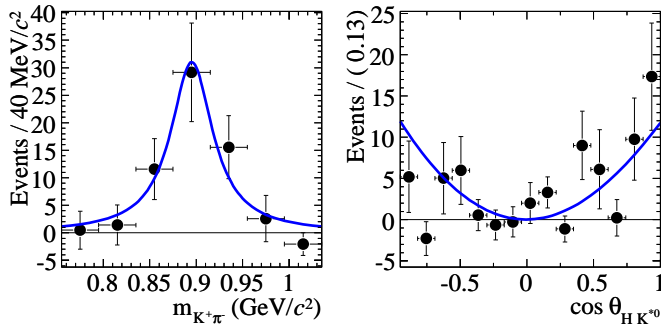


FIG. 2: (Color online) Distributions of the $K\pi$ mass (*left*) and helicity (*right*) for the decay $B^0 \rightarrow \eta' K^{*0}$. Points with error bars: data, background subtracted with the sPlot technique, solid curve: signal PDF.

fractions (3.4%). Uncertainties in the event selection efficiency are 0.5–3% for the requirement on $\cos \theta_T$.

We assign a systematic uncertainty on \mathcal{A}_{ch} of 0.02, based on studies of inclusive samples of kaons and B decays. This is due primarily to asymmetries in charged kaon identification and slow pion reconstruction.

We present measurements for the decays $B^{+,0} \rightarrow \eta' K^{*+,0}$ and $B^+ \rightarrow \eta' \rho^+$. They allow the level of suppression of these decays, with respect to the enhanced $\eta' K$ and ηK^* , to be determined. A simultaneous fit of all charged and neutral $\eta' K^*$ submodes results in the observation of $B \rightarrow \eta' K^*$ with a total significance of 5.6σ , including systematics, as shown in Table I. The measurements place constraints on possible enhanced flavor-singlet contributions to these decays [2, 15]. These results are consistent with previous upper limits, where they existed. In all cases, predictions based on SU(3) flavor symmetry [4], QCD factorization [5] and perturbative QCD [6] are in excellent agreement with our measured central values. Values of \mathcal{A}_{ch} are consistent with zero in all channels.

We are grateful for the excellent luminosity and machine conditions provided by our PEP-II colleagues, and for the substantial dedicated effort from the computing organizations that support *BABAR*. The collaborating institutions wish to thank SLAC for its support and

kind hospitality. This work is supported by DOE and NSF (USA), NSERC (Canada), IHEP (China), CEA and CNRS-IN2P3 (France), BMBF and DFG (Germany), INFN (Italy), FOM (The Netherlands), NFR (Norway), MIST (Russia), MEC (Spain), and PPARC (United Kingdom). Individuals have received support from the Marie Curie EIF (European Union) and the A. P. Sloan Foundation.

* Also at Laboratoire de Physique Corpusculaire, Clermont-Ferrand, France

† Also with Università di Perugia, Dipartimento di Fisica, Perugia, Italy

‡ Also with Università della Basilicata, Potenza, Italy

- [1] B. Aubert *et al.* (*BABAR*), Phys. Rev. Lett. **94**, 191802 (2005).
- [2] M. Beneke and M. Neubert, Nucl. Phys. B **651**, 225 (2003).
- [3] H. J. Lipkin, Phys. Lett. B **254**, 247 (1991).
- [4] C.-W. Chiang *et al.*, Phys. Rev. D **69**, 034001 (2004).
- [5] M. Beneke and M. Neubert, Nucl. Phys. B **675**, 333 (2003).
- [6] X. Liu *et al.*, Phys. Rev. D **73**, 074002 (2006).
- [7] B. Aubert *et al.* (*BABAR*), Nucl. Instrum. Meth. **A479** (2002).
- [8] B. Aubert *et al.* (*BABAR*), Phys. Rev. D **70**, 032006 (2004).
- [9] B. Aubert *et al.* (*BABAR*), Phys. Rev. Lett. **94**, 161803 (2005).
- [10] S. Eidelman *et al.* (Particle Data Group), Phys. Lett. B **592**, 1 (2004).
- [11] The *BABAR* detector Monte Carlo simulation is based on GEANT4: S. Agostinelli *et al.*, Nucl. Instrum. Meth. **A506**, 250 (2003).
- [12] E. M. Aitala *et al.* (FNAL E791), Phys. Rev. Lett. **86**, 765 (2001).
- [13] M. Pivk and F. R. Le Diberder, Nucl. Instrum. Meth. **A555**, 356 (2005).
- [14] B. Aubert *et al.* (*BABAR*), Phys. Rev. D **67**, 032002 (2003).
- [15] C.-W. Chiang and J. L. Rosner, Phys. Rev. D **65**, 074035 (2002).